DOI: 10.1002/ejoc.201000037

On the Tautomerism of Secondary Phosphane Oxides

Andrea Christiansen,[a,b] Chuanzhao Li,[c] Marc Garland,[c] Detlef Selent,[a] Ralf Ludwig,[d] Anke Spannenberg,[a] Wolfgang Baumann,[a] Robert Franke,[b] and Armin Börner*[a,d]

Dedicated to Uwe Rosenthal on the occasion of his 60th birthday

Keywords: Phosphorus / Tautomerism / NMR spectroscopy / IR spectroscopy

The tautomeric behaviour of five secondary phosphane oxides (SPOs) with different electronic properties has been investigated by NMR and IR spectroscopy, density functional theory calculations and X-ray structural analysis. Proof is given that only with strong electron-withdrawing groups on the phosphorus atom can the relevant trivalent phosphinous acid be observed in the equilibrium, whereas in the case of electron-rich phosphane oxides the pentavalent species dominates. For a detailed analysis of the IR spectra, the deconvolution programme BTEM has been successfully applied.

Introduction

As a result of their versatility and modular synthesis, trivalent phosphorus compounds such as phosphanes, phosphinites, phosphonites and phosphites represent the most commonly used classes of ancillary ligands in homogeneous catalysis.[1] Owing to the presence of the free electron pair they are able to coordinate to a metal centre. However, pentavalent phosphorus compounds can also be considered as potential ligands, provided there is an equilibrium with trivalent phosphorus species as constituents.

In this respect, secondary phosphane oxides, abbreviated as SPOs (R = alkyl, aryl), or heteroatom-substituted secondary phosphane oxides, abbreviated as HASPOs (at least one R = NR''_2 or OR''), are of particular interest (**A**, Scheme 1).[2]

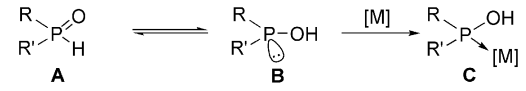

Scheme 1. Tautomeric equilibrium of pentavalent and trivalent phosphorus compounds and the formation of metal complexes.

(HA)SPOs **A** are weak acids.[3] Therefore, they can tautomerize in solution to phosphinous acids **B**.[4] The latter are trivalent, and thus they are able to bind to a metal centre to give metal complexes **C**. As a result, we recently suggested the term preligands.[5] Indeed, several examples have been reported in the literature in which (HA)SPOs have been successfully used as ancillary ligands in homogeneous metal-catalyzed reactions.[6,7]

In spite of these applications in catalysis little is known about the chemical and physical properties of the desmotrope depicted in Scheme 1 even though this information is crucial for an assessment of their coordination behaviour and ultimately their catalytic properties. In general, (HA)SPOs are reputed to be stable towards oxygen, which has been explained by the dominance of the pentavalent tautomer **A** in solution.[8] It is assumed that the equilibrium is only shifted towards the trivalent tautomer **B** in the presence of a metal centre.

Already in the 1960s, secondary phosphonates, phosphinates and phosphane oxides were being examined in deuterium exchange[9] and oxidation[9c,10] reactions.[3a] The results of these investigations suggested that the pentavalent species is dominant in most instances. Preliminary IR spectroscopic measurements confirmed the formal P=O nature of alkyl- and aryl-substituted SPOs.[11] Pietrusiewicz and Duddeck and their co-workers suggested that the tautomeric equilibrium forms rapidly because the migration of an (acidic) proton is involved.[12] Recent DFT calculations by Ustynyuk and Babin revealed that an intramolecular proton transfer is not favoured due to high activation barriers.[13] In the absence of a proton carrier, as in non-polar media, the rearrangement proceeds as a synchronous trans-

[a] Leibniz-Institut für Katalyse an der Universität Rostock e.V., A.-Einstein-Str. 29a, 18059 Rostock, Germany
Fax: +49-381-1281-51202
E-mail: armin.boerner@catalysis.de
[b] Evonik Oxeno GmbH, Paul-Baumann-Straße 1, 45772 Marl, Germany
[c] Institute of Chemical and Engineering Sciences, 1 Pesek Road, Jurong Island, 627833 Singapore
[d] Institut für Chemie der Universität Rostock, A.-Einstein-Str. 3a, 18059 Rostock, Germany

fer of two protons in dimeric associates. However, systematic studies on this tautomerism have not been available until now.

For our study we chose five related SPOs **1**–**5** possessing P substituents with electron-donating or -withdrawing properties. Recently, the pertinent equilibria for $(OH)_2P(O)H$[14] and (*t*Bu)PhP(O)H[15] were studied theoretically. The seminal work was performed by Hoge et al. who investigated electronically poor SPOs and found a solvent-dependent shift of the tautomeric equilibria.[16] In addition, for compound **5** the zero-point-corrected energy difference ΔE_{ZPE} between both tautomers was calculated.

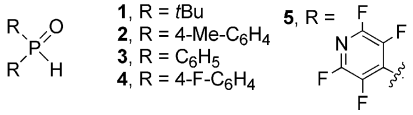

To widen the scope of these investigations, herein we wish to present our studies on the tautomeric equilibria of SPOs **1**–**5** based on NMR spectroscopic characterization, investigations on the influence of solvent and temperature, DFT calculations, X-ray structural analysis and IR spectroscopic characterization.

Results and Discussion

NMR Spectroscopic Investigations

Correlation of the ^{31}P NMR Shifts and ^{31}P–^{1}H Coupling Constants

Investigations of the SPOs **1**–**5** in CD_2Cl_2 by ^{31}P NMR spectroscopy revealed that with the exception of the perfluorinated compound **5** at ambient temperature all other SPOs exist exclusively in the pentavalent tautomeric form **A** (Scheme 1). The experimentally determined chemical shifts ($\delta^{31}P$) and ^{31}P–^{1}H couplings (J_{P-H}) are depicted in Figures 1 and 2. For comparison, the calculated values are also given.[17]

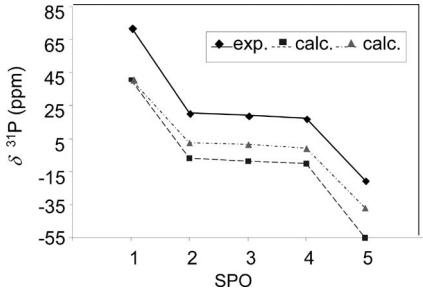

Figure 1. Plot of the ^{31}P NMR chemical shifts (δ) of the P=O tautomers of **1**–**5**: experimentally determined in CD_2Cl_2 (top) and calculated at the B3LYP/6-31+G* (middle) and B3LYP/6-311+G* levels of theory (bottom).

As can clearly be seen, electron-withdrawing substituents, which decrease the Lewis basicity of the phosphorus atom, cause a shift to higher field and an enhancement in the P–H couplings. The quantum chemical calculations confirm this trend. In general, the electronic differences between the phenyl-substituted compounds are small. This is also revealed in Figure 3.

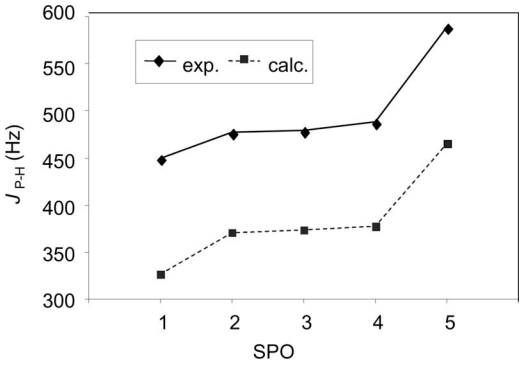

Figure 2. Plot of the P–H coupling constants of the P=O tautomers **1**–**5** in the ^{31}P NMR spectrum: experimentally determined (in CD_2Cl_2) (top) and calculated at the B3LYP/6-31+G* level of theory (bottom).

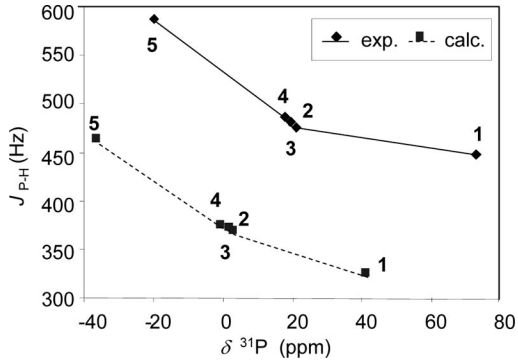

Figure 3. Correlation of the P–H coupling constants versus chemical shifts in the ^{31}P NMR spectrum of the P=O tautomers of **1**–**5**: experimentally determined (in CD_2Cl_2) (top) and calculated at the B3LYP/6-31+G* level of theory (bottom).

Influence of the Solvent

As the tautomeric equilibrium of electron-poor SPO **5** in dichloromethane displayed besides the phosphane oxide **A** also the phosphinous acid **B** (ratio 59:41), this SPO was first chosen to investigate the effect of solvent on the shift of the tautomeric equilibrium. Although the pentavalent tautomer **A** predominates in the equilibrium in $[D_8]$toluene and CD_2Cl_2 with a ratio of 59:41, in more polar solvents like $[D_8]$THF and CD_3OD the equilibrium is shifted completely to the phosphinous acid **B** (Table 1).

Clearly the trivalent tautomer **5B** is "stabilized" by polar solvents. Surprisingly, this remarkable solvent dependency was not observed for SPOs **1**–**4**. The relevant trivalent tautomers **B** were not detected in toluene, THF, dichloromethane or trifluoroethanol. In each case only a single signal characterizing the pentavalent tautomer was found. In deuteriated methanol as well as in trifluoroethanol, exchange of the *P*-bonded proton by deuterium took place. It is assumed that this reaction is reversible.[9f] Esterification with the alcoholic solvent did not take place with SPOs **1**–**4**. In

Table 1. Tautomeric equilibrium of bis(tetrafluoropyridyl)phosphane oxide (**5**) at room temperature according to a ^{31}P NMR analysis.

Solvent	Ratio **A/B**
[D_8]Toluene	59:41
CD_2Cl_2	59:41
[D_8]THF	0:100
CD_3OD	0:100[a]
[D_8]Toluene/CD_3OD (3:1)	0:100
[D_8]Toluene/CF_3CD_2OD (3:1)	81:19
CF_3CD_2OD	87:13

[a] Measurement after 60 min; P–OD tautomer **B** corresponds to only 8.8% of the overall signal intensity due to degradation reactions with CD_3OD.

contrast, in deuteriated methanol or in mixtures of methanol/toluene, SPO **5** was converted rapidly. The corresponding methyl ester and several decomposition products were observed, characterized by signals in the ^{31}P NMR spectrum between δ = +10 and –10 ppm. This observation indicates that the solvent does not only influence the state of the tautomeric equilibrium, but may also contribute to the degradation of SPOs.

Clearly the polarity of the solvent is not the only reason for the shift in the equilibrium observed. Thus, although the polarity of THF is classified as being between toluene and dichloromethane,[18] the ratio of tautomers **A/B** does not reflect this order. Moreover, in trifluoroethanol, which displays a much higher polarity than methanol, surprisingly, the pentavalent tautomer **5A** dominates the equilibrium. This effect can be rationalized by taking the hydrogen-bonding acceptor properties of the solvent into consideration. Whereas methanol and THF exhibit strong hydrogen-bonding acceptor properties, trifluoroethanol, toluene and CH_2Cl_2 are rather poor hydrogen-bonding acceptors.[18] Hence, more than the polarity of solvents, their hydrogen-bonding acceptor properties affect the state of the tautomeric equilibria of secondary phosphane oxides.

When diphenylphosphane oxide (**3**) was dissolved in a mixture of $CDCl_3$ and [D_6]acetone we observed, besides the pentavalent P=O tautomer **A** (δ = 22.8 ppm), the formation of a second species characterized by a resonance at δ = 32.4 ppm. Analysis of the ^{13}C NMR spectrum, the reaction with non-deuteriated acetone and a comparison with literature data[19] revealed that the trivalent tautomer **3B** was not formed,[20] but *P*-(2-hydroxyisopropyl)diphenylphosphane oxide (**6**; Scheme 2). This compound derives from the addition of **3B** to acetone, similar to that recently described by Hoge et al. for the reaction of $(C_6F_5)_2P(O)H$.[16]

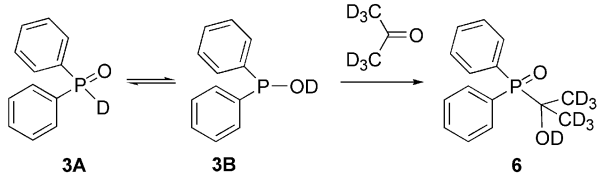

3A 3B 6

Scheme 2. Reaction of SPO **3** with [D_6]acetone.

Influence of Temperature

To evaluate the temperature dependency of the equilibria, dynamic NMR measurements were performed. SPOs **1**–**3** and **5** were investigated in a temperature range of –80 to +55 °C. Although at room temperature for compounds **1**–**3** only the corresponding phosphane oxide could be detected (see above), we assume an infinitesimally small amount of the phosphinous acid to be present and to contribute to the P–H coupling constant. Thus, the measured coupling constants represent an average value derived from Equation (1).

$$J_{average} = x^2J(P–OH) + (1–x)^1J(P–H) \quad (1)$$

This equation is only valuable under the precondition that a fast exchange between the P–H and P–OH species takes place. According to Equation (1), a change in the coupling constant can be attributed to a shift in the tautomeric equilibrium. With THF as solvent for SPOs **1**–**3** only a small decrease in the P–H coupling was observed (in the range of 6–9 Hz) by increasing the temperature, which indicates a slight shift in the equilibria in favour of the trivalent tautomer. Unfortunately, the latter could not be detected in the spectrum, apparently because of the poor sensitivity of the analytical method applied.

The question arises as to whether there is a temperature dependency of the P–H coupling constants as a matter of principle. Thus, a sample of bis(*p*-tolyl)phosphane, $(CH_3C_6H_4)_2PH$, was cooled from room temperature to –80 °C, and an increase in $J_{P–H}$ of 2 Hz was observed. This means that the previously measured data with $\Delta J_{P–H}$ = 6–9 Hz for SPOs **1**–**3** have to be corrected on average by 2–4 Hz. The resulting differences in the coupling constants are only marginal so that an influence of the temperature on the equilibria can be neglected.[21]

When the equilibrium of electron-poor SPO **5** was investigated in toluene (in which both tautomers coexist) in the temperature range –80 to +55 °C, a shift in the tautomeric equilibrium in favour of the trivalent tautomer took place, as demonstrated by a shift in the signal intensities of both tautomers by about 6%. Quantum chemical calculations of the equilibrium constant carried out for –100 and +55 °C at the B3LYP/6-31+G* level of theory also indicated a change of 7%, which agrees well with the experimentally determined value. However, taking the large temperature interval into consideration this contribution can be neglected.

DFT Calculations and X-ray Structural Analysis

As NMR spectroscopy is not powerful enough to quantify the state of the tautomeric equilibria of ligands **1**–**4**, DFT calculations were performed by using the Gaussian 03 software package[22] with the B3LYP functional[23] to determine whether electronic variations at the *para* position of phenyl substituents in secondary phosphane oxides influence the tautomeric equilibria or not. The results are listed in Table 2. In a first step, the individual structures of the

tautomers were optimized at the B3LYP/6-31G* level of theory. For the optimized structures, frequency calculations were performed to ensure that they are local minima and to yield zero-point vibrational energies and Gibbs free energies that include their thermal corrections at 298 K. Subsequently, the structures obtained were further optimized at the B3LYP/6-311+G* level of theory. The free enthalpy (G) was finally calculated by using the electronic energies (E_{tot}) at the B3LYP/6-311+G* level and by employing zero-point vibrational energies as well as statistical thermodynamic contributions obtained at the B3LYP/6-31G* level of theory.

Table 2. Calculated differences in the free enthalpy of the tautomers of **1**–**5** in the relevant equilibria in the gas phase.

	Tautomer **A**				
	1	**2**	**3**	**4**	**5**
ΔG(**A**–**B**) [kJ/mol]	–31.17	–16.53	–12.64	–10.88	+16.74
Share of **A** [%]	>99.99	>99.87	>99.27	>98.78	<0.01

The state of the equilibrium between the pentavalent and trivalent isomers can be calculated from the free enthalpies according to $\Delta G = -RT\ln K$ in which K = [**A**]/[**B**] and [**B**] = 100 – [**A**].

In agreement with the experimental data, the pentavalent tautomer **A** in SPOs **1**–**4** is much more stable than the trivalent form, and therefore it dominates the equilibria of **1**–**4**. In contrast, for the electron-poor compound **5**, the phosphinous acid **B** is stabilized by 16.74 kJ mol^{-1} with respect to the corresponding oxide form. Hence, the equilibrium is shifted towards the trivalent P–OH form. The calculated state of the equilibria of SPOs **1**–**5** conform to those determined by NMR spectroscopy in a THF solution.

For SPO **2** the structure of the pentavalent tautomer was additionally evidenced by X-ray structural analysis. The solid-state structure as well as distances and angles are given in Figure 4. The calculated data fit well with those obtained by structural analysis. According to both methods the P–O distance is characteristic of a formal P=O double bond.

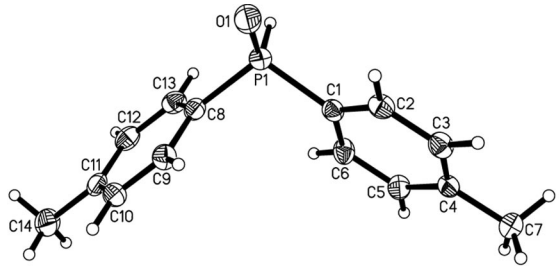

SPO **2**	P=O [Å]	P–C [Å]	C–P–C [°]
Determined by X-ray crystallography	1.471(2)	1.799(2), 1.793(2)	107.13(6)
Determined by DFT calculation	1.4985	1.8204, 1.8245	107.05

Figure 4. Molecular structure of **2A** with selected bond lengths and angles and comparison with the calculated data.[24]

Calculations of the structures of the trivalent phosphinous acids **B** of **1**–**5** gave two minima in each case, which is in accordance with the existence of rotational P–OH isomers. Already in 1971, Dobbie and Straughan observed two OH stretching vibrations for gaseous $(CF_3)_2POH$ in the IR spectrum and suggested the coexistence of rotational isomers.[25] These observations were recently confirmed by DFT calculations by Hoge et al.[26]

Thereupon we calculated the potential energy curves for compounds **1**–**5** along the C–P–O–H dihedral angle and obtained two minima in each case. Exemplary results for diphenylphosphinous acid (**3B**) and bis(tetrafluoropyridyl) phosphinous acid (**5B**) are depicted in Figures 5 and 6.[27] The energy difference calculated for Ph_2POH (**3B**) is 14.18 kJ mol^{-1}, whereas the difference in the minima calculated for $(C_5NF_4)_2POH$ (**5B**) is much smaller (6.50 kJ mol^{-1}).[28]

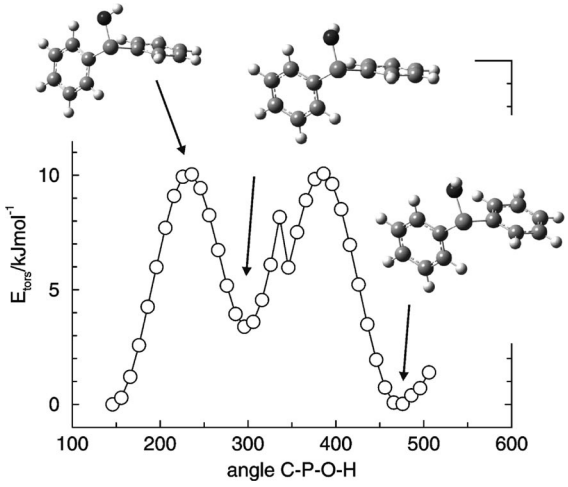

Figure 5. Torsion potential of Ph_2POH (**3B**) along the C–P–O–H dihedral angle (calculated at the B3LYP/6-31+G* level).

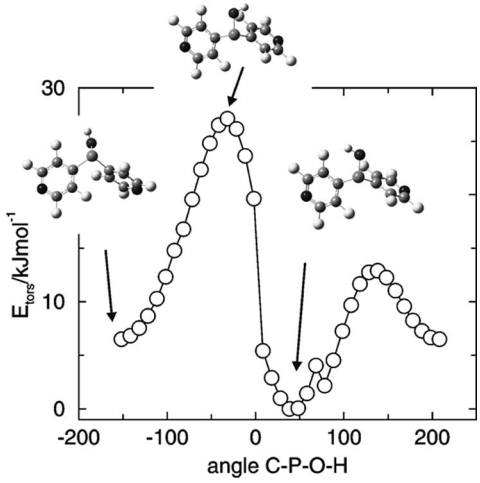

Figure 6. Torsion potential of $(C_5NF_4)_2POH$ (**5B**) along the C–P–O–H dihedral angle (calculated at the B3LYP/6-31+G* level).

IR Spectroscopic Studies

The tautomeric equilibria of the SPOs can also be determined by IR spectroscopy by taking advantage of the characteristic P–H, O–H and P–O vibrational bands. We started by calculating the IR spectra using DFT. The calculated absorption bands of the relevant pentavalent tautomers of type **A** are depicted in Figure 7.

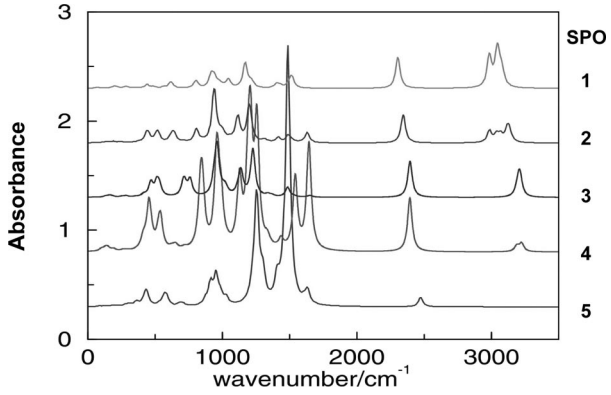

Figure 7. Calculated IR spectra of the pentavalent tautomers **A** of SPOs **1**–**5** (at the B3LYP/6-31+G* level).

Clearly, the P–H vibration ($\tilde{\nu}_{PH}$ in the range of ca. 2300–2500 cm^{-1}) is particularly valuable for kinetic studies because there are no overlapping signals in this region in contrast to the P–O area.

Figure 8 shows a comparison between the experimentally obtained and calculated P–H vibrational bands of SPOs **1**–**5**.[29,30] There is a difference in the values obtained by the two methods because the calculations were carried out in a harmonic approximation, whereas in experiments anharmonic contributions also play a role. Irrespective of this feature, a general trend similar to the P–H coupling constants in the NMR analysis can be observed: strong electron-accepting substituents at the phosphorus atom enhance $\tilde{\nu}_{PH}$.

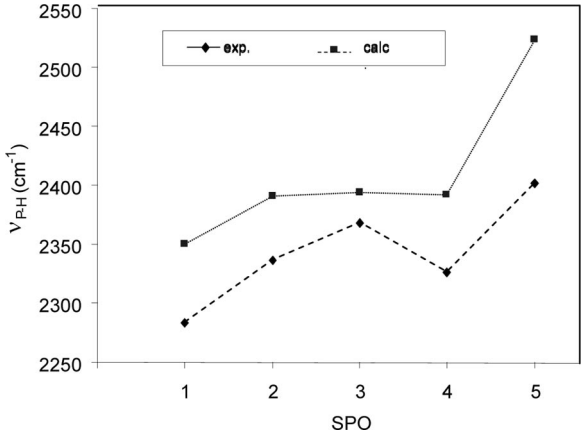

Figure 8. Experimentally obtained (bottom; in KBr, compound **5** measured by means of ATR) and calculated (top; calculated at the B3LYP/6-31+G* level) P–H vibrational bands of compounds **1**–**5**.

The DFT calculations described above reveal that the phosphinous acids **B** exist as two rotational isomers that exhibit different interactions between the OH groups and the other *P*-substituents. This feature leads to distinct OH bands, as exemplarily shown for di-*tert*-butylphosphane oxide (**1**) in Figure 9. Therefore, the state of the equilibrium cannot be determined just by integrating the $\tilde{\nu}_{PH}$ and $\tilde{\nu}_{OH}$ bands.

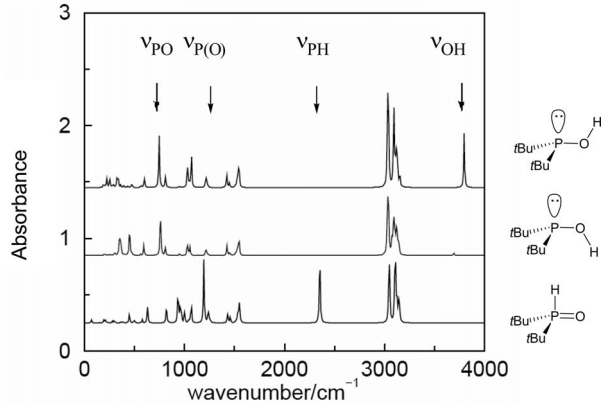

Figure 9. IR spectra of the calculated rotational isomers (top and middle) as well as of the pentavalent tautomer (bottom) of desmotrope **1** (at the B3LYP/6-31+G* level).

However, a reliable conclusion can be derived by comparison of the signal area of the $\tilde{\nu}_{PO}$ bands. To identify these pivotal resonances deconvolution of the experimentally measured IR spectra is required owing to overlapping signals. Exemplarily, the BTEM algorithm was applied to deconvolute the spectra of bis(tetrafluoropyridyl)phosphane oxide (**5**) and diphenylphosphane oxide (**3**).[31]

Bis(tetrafluoropyridyl)phosphane Oxide (5)

Full-range deconvolutions of $(C_5NF_4)_2P$–OH (**5**) in toluene and [D_6]benzene are shown in Figure 10. The BTEM spectral estimate in toluene (Figure 10a) clearly shows the O–H vibration, but not the P–O band.[32] In contrast, the spectral estimate in [D_6]benzene (Figure 10b) shows not only the O–H band, but also the very intense P–O vibration at 1456 cm^{-1}.

As discussed above, the NMR spectroscopically determined tautomeric equilibrium for perfluorinated SPO **5** in toluene is 59:41 [P(O)H/P–OH] at room temperature. DFT calculations predicted the presence of two rotational isomers, which could not be observed in the NMR spectra even at 200 K. Accordingly, BTEM analysis was reapplied to the spectroscopic data in a narrower range, specifically 3250–3800 cm^{-1}. Two spectral estimates were obtained that have band maxima at 3470 (Figure 11a) and 3434 cm^{-1} (Figure 11b). The difference $\tilde{\nu}_{OH\_1} - \tilde{\nu}_{OH\_2} = 36$ cm^{-1} is in good agreement with the value of 38 cm^{-1} obtained by DFT calculations. To the best of our knowledge, the present deconvolution has enabled the first observation of two simultaneous P–OH rotational isomers in the liquid phase by IR spectroscopy.

BTEM analysis was reapplied to the spectral range 2086–3800 cm^{-1} to identify the P–H stretching vibration of the pentavalent tautomer **5A**. As shown in Figure 12, one pure-component spectrum was recovered in which a P–H vi-

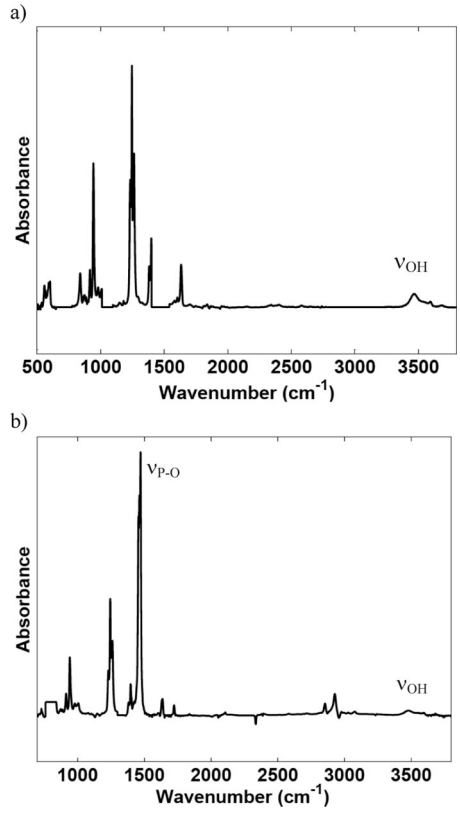

Figure 10. Vibrational spectrum of $(C_5NF_4)_2P$–OH (**5B**) after deconvolution with BTEM in (a) toluene and (b) [D_6]benzene by using the full range of spectroscopic data.

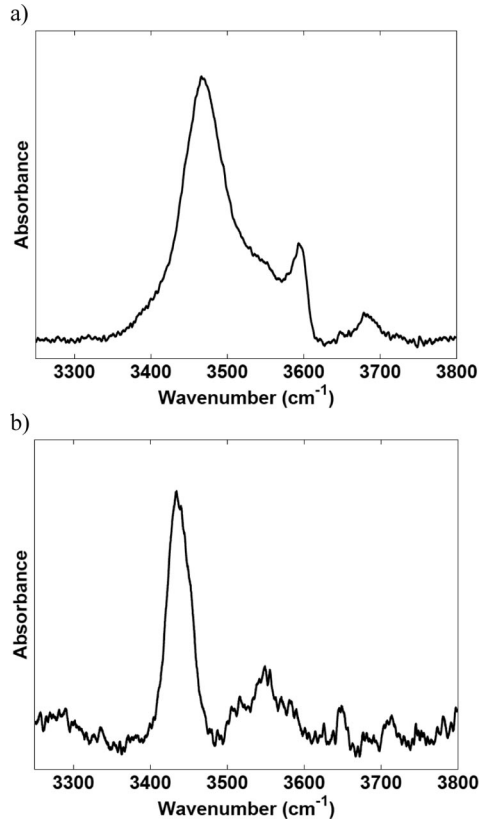

Figure 11. BTEM spectral estimates of the $\tilde{\nu}_{OH}$ band of the two rotational isomers of $(C_5NF_4)_2P$–OH (**5B**) in toluene.[33]

bration is correlated with the O–H vibration at 3470 cm^{-1}. Owing to the weak intensity of the P–H vibrations, a second spectral estimate could not be obtained.

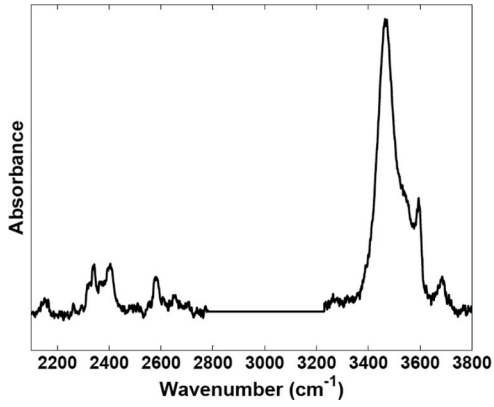

Figure 12. A BTEM spectral estimate showing correlated O–H and P–H regions for the desmotrope of SPO **5**.

According to the NMR spectroscopic investigations the pentavalent tautomer **A** of **3** dominates the equilibrium. A full-range deconvolution of **3** by using BTEM is shown in Figure 13a.

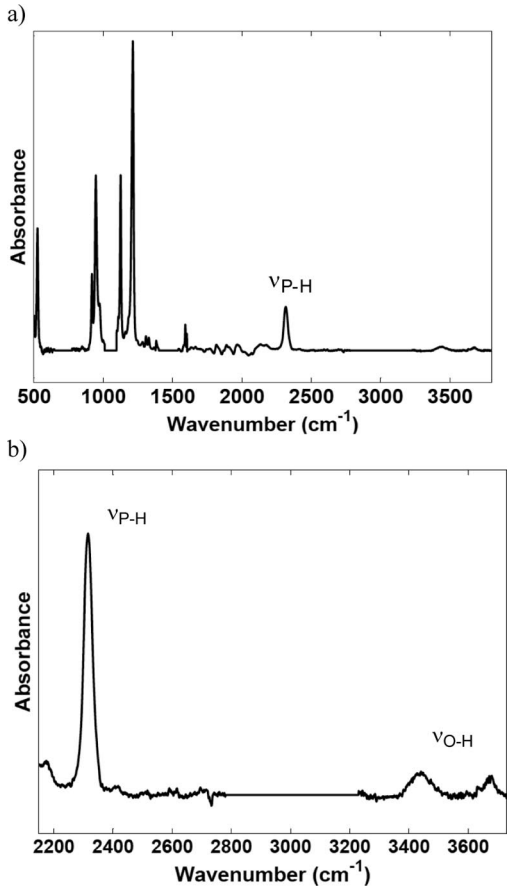

Figure 13. IR spectra of $(C_6H_5)_2P(O)H$ (**3**) in toluene after deconvolution with BTEM (target ν_{P-H}): (a) whole range and (b) section showing the O–H and P–H vibrations.

In contrast to the results obtained with SPO **5**, the spectral estimate for **3** shows a pronounced P–H vibration at 2312 cm^{-1}. A subsequent analysis with BTEM was performed in the narrower region 2086–3800 cm^{-1}. The spectral estimate (Figure 13b) displays an intense P–H vibration as well as vibrations in the O–H region. Therefore, this region was analysed with BTEM to look for the rotational isomers of the trivalent tautomer. However, this gave rise to the same spectrum as that obtained for the pentavalent P(O)–H tautomer in Figure 13a. Apparently, bands of the phosphane oxide and the phosphinous acid are superimposed in the same spectrum, as already shown for compound **5**.

Conclusions

The tautomeric equilibria of five secondary phosphane oxides have been investigated by NMR and IR spectroscopy as well as by quantum chemical calculations. Solvent dependency based on the hydrogen-bond acceptor properties rather than on the polarity of solvents was demonstrated for SPO **5**. The solvent not only influences the state of the tautomeric equilibrium, but may also contribute to the degradation of SPOs, for example, esterification. A strong influence of temperature on the state of the equilibria can be ruled out.

The influence of electron-withdrawing substituents, which decrease the Lewis basicity of the phosphorus atom, is reflected by the phosphorus chemical shifts in the NMR spectra. Electron-withdrawing substituents cause an enhancement of the P–H couplings and a shift to higher fields. Similarly, in IR spectroscopy, electron-accepting substituents enhance $\tilde{\nu}_{PH}$. The state of the equilibria between the pentavalent and trivalent isomers of the SPOs **1**–**5** was calculated from the free enthalpies. They conform to those determined by NMR spectroscopy in a THF solution.

For SPO **2** the structure of the pentavalent tautomer was additionally evidenced by X-ray structural analysis.

DFT calculations revealed that phosphinous acids of type **B** exist as two rotational isomers. Indeed, the presence of rotational isomers for $(C_5NF_4)_2P$–OH (**5B**) and Ph_2P–OH (**3B**) has been evidenced by IR spectroscopy for the first time in the liquid phase. The identification of both tautomers of compounds **3** and **5** by IR spectroscopy is the precondition for the quantitative evaluation of their tautomeric equilibria. Next, we will focus on the establishment of time-dependent concentration profiles with the aim of tracking the equilibria during the complexation of SPOs to metal centres.

Experimental Section

General Procedures: Unless stated otherwise, all reactions were carried out under argon 5.0 by using standard Schlenk techniques. Commercially available compounds were used as purchased. Solvents were dried by conventional procedures and distilled under argon. Where possible, reactions were monitored by NMR spectroscopy. The yields listed below are isolated yields. NMR spectra were recorded with Bruker AV 300 and AV 400 spectrometers. Chemical shifts are reported in ppm relative to deuteriated solvents. TMS was used as the standard in ^1H and ^{13}C NMR spectra and H_3PO_4 in ^{31}P NMR spectra. Mass spectra were recorded with an AMD 402 spectrometer and IR spectra with a Nicolet Magna-IR 550 spectrometer. Elemental analyses were performd with a LECO CHNS-932. Melting points were determined with Stuart SMP 3.

BTEM Analysis: Around 300 spectra were measured for each experimental run. Each set was analysed individually by using the BTEM algorithm to provide pure-component spectra of the components present. Details of the BTEM algorithm are provided elsewhere.[34] Because the toluene and benzene solvents absorb strongly in some regions, spectroscopic data in these regions were deleted prior to BTEM analyses. BTEM analysis was then conducted on three regions of data: (1) 500–3800 cm^{-1} for full-range deconvolutions, (2) 2086–3800 cm^{-1} for deconvolutions focused on the P–H and O–H vibrations and (3) 3250–3800 cm^{-1} for deconvolutions focused on O–H vibrations.

Di-*tert*-butylphosphane Oxide (1): Strem, 98%. ^1H NMR (300 MHz, CD_2Cl_2): δ = 6.17 (d, J_{P-H} = 449.8 Hz, 1 H, PH), 1.29 [d, J = 16.0 Hz, 18 H, $C(CH_3)_3$] ppm. ^{13}C NMR (75 MHz, CD_2Cl_2): δ = 33.8 [d, J = 58 Hz, $C(CH_3)_3$], 25.4 [d, J = 2 Hz, $C(CH_3)_3$] ppm. ^{31}P NMR (121 MHz, CD_2Cl_2): δ = 72.4 ppm. IR (KBr): $\tilde{\nu}$ = 2284 (P–H) cm^{-1}.

Di(*p*-tolyl)phosphane Oxide (2): Usually, SPO **2** is synthesized by Grignard reaction of di(*p*-tolyl)magnesium bromide with diethyl phosphite and HCl.[36] For small amounts the following procedure is more useful. 2-Propanol (25 mL) was added under constant stirring to bis(4-methylphenyl)phosphane (2.145 g, 932 mmol) at ambient temperature. The solution was kept at 50 °C and stirred in an open flask for 90 min. The solvent was distilled in vacuo and the residue dissolved in dry, boiling diethyl ether (30 mL). On cooling to room temperature the product precipitated as a white solid. The product was recrystallized from diethyl ether to remove unreacted phosphane. Colourless needles (1.42 g, 62%) suitable for X-ray crystallography were obtained, which proved to be air-stable for several weeks. M.p. 95–96 °C (Et_2O). ^1H NMR (300 MHz, CD_2Cl_2): δ = 7.98 (d, J_{P-H} = 477.3 Hz, 1 H, PH), 7.54 (m, 4 H, C_6H_4), 7.30 (m, 4 H, C_6H_4), 2.39 (s, 6 H, CH_3) ppm. ^{13}C NMR (75 MHz, CD_2Cl_2): δ = 143.4 (d, J = 2.8 Hz, C_6H_4, CCH_3), 130.8 (d, J = 11.7 Hz, CH, C_6H_4), 129.8 (d, J = 13.0 Hz, CH, C_6H_4), 129.3 (d, J = 103.2 Hz, C_6H_4, CP), 21.6 (d, J = 1.2 Hz, CH_3) ppm. ^{31}P NMR (121 MHz, CD_2Cl_2): δ = 20.5 ppm. ^1H NMR (300 MHz, [D_8]THF): δ = 7.99 (d, J_{P-H} = 477.8 Hz, 1 H, PH), 7.61–7.48 (m, 4 H, C_6H_4), 7.35–7.26 (m, 4 H, C_6H_4), 2.39 (s, 6 H, CH_3) ppm. ^{31}P NMR (121 MHz, [D_8]THF): δ = 20.6 ppm. IR (KBr): $\tilde{\nu}$ = 2337 (P–H) cm^{-1}. $C_{14}H_{15}OP$ (230.25): calcd. C 73.03, H 6.57, P 13.45; found C 73.1, H 6.55, P 13.58.

Diphenylphosphane Oxide (3): Aldrich, >97%. ^1H NMR (300 MHz, CD_2Cl_2): δ = 8.05 (d, J_{P-H} = 480.1 Hz, 1 H, PH), 7.69 (m, 4 H, C_6H_5), 7.54 (m, 6 H, C_6H_5) ppm. ^{13}C NMR (76 MHz, CD_2Cl_2): δ = 132.7 (d, J = 2.8 Hz, C_6H_5, C-4), 132.4 (d, J = 100.6 Hz, CP), 130.8 (d, J = 11.4 Hz, C_6H_5, C-2), 129.1 (d, J = 12.5 Hz, C_6H_5, C-3) ppm. ^{31}P NMR (122 MHz, CD_2Cl_2): δ = 20.4 ppm. ^{31}P NMR (122 MHz, CD_3OD): δ = 24.5 (d, $^1J_{P-H}$ = 495.4 Hz), 23.9 (t, $^1J_{P-D}$ = 75.7 Hz) ppm. ^{31}P NMR (162 MHz, CF_3CD_2OD): δ = 29.6 (d, $^1J_{P-H}$ = 498.5 Hz), 29.0 (t, $^1J_{P-D}$ = 76.3 Hz) ppm. IR (KBr): $\tilde{\nu}$ = 2368 (P–H) cm^{-1}.

Bis(4-fluorophenyl)phosphane Oxide (4): *tert*-Butyl alcohol (20 mL) was added to bis(4-fluorophenyl)chlorophosphane (5 mL, Digital Speciality Products, 98.5%) under constant stirring.[37] The Schlenk

tube was sealed. After 6 min of stirring at room temperature, the volatiles were removed in vacuo, and the product was obtained quantitatively as a viscous liquid. It should be stored below 10 °C to prevent disproportionation into R_2PH and $R_2P(O)OH$ (R = 4-F-C_6H_4). ^1H NMR (400 MHz, CD_2Cl_2): δ = 8.06 (d, J_{P-H} = 488.60 Hz, 1 H, PH), 7.67 (m, 4 H, C_6H_4), 7.09 (m, 4 H, C_6H_4) ppm. ^{13}C NMR (101 MHz, CD_2Cl_2): δ = 165.1 (dd, J = 3.3, J = 252.9 Hz, CF), 133.1 (dd, J = 8.9, J = 13.1 Hz, C_6H_4), 128.0 (dd, J = 3.4, J = 103.3 Hz, CP), 116.1 (dd, J = 13.9, J = 21.6 Hz, C_6H_4) ppm. ^{19}F NMR (282 MHz, CD_2Cl_2): δ = –106.0 (m) ppm. ^{31}P NMR (162 MHz, CD_2Cl_2): δ = 17.5 ppm. IR (KBr): $\tilde{\nu}$ = 2327 (P–H) cm^{-1}. MS (EI, 70 eV): m/z = 237 $[M]^+$. $C_{12}H_9F_2OP$ (238.17): calcd. C 60.51, H 3.81, P 13.00; found C 60.53, H 3.86, P 13.03.

Bis(tetrafluoropyridyl)phosphane Oxide (5): This compound was synthesized by Hoge et al.[16] and generously provided for our research. ^1H NMR (400 MHz, [D$_8$]THF): δ = 9.00 (br., 1 H, POH) ppm. ^{13}C NMR (101 MHz, [D$_8$]THF): δ = 144.5–141.9 (m, C_5NF_4) ppm. ^{19}F NMR (282.4 MHz, [D$_8$]THF): δ = –92.9 (m), –137.1 (m) ppm. ^{31}P NMR (162 MHz, [D$_8$]THF): δ = 71.8 (quint, J_{P-F} = 26.9 Hz, POH) ppm. ^1H NMR (300 MHz, [D$_8$]toluene): δ = 7.87 (d, J_{P-H} = 585.5 Hz, PH), 4.78 (br., POH) ppm. ^{19}F NMR (282.4 MHz, [D$_8$]toluene): δ = –86.6 [m, P(O)H], –89.9 (m, POH), –135.1 [m, P(O)H], –136.4 (m, POH) ppm. ^{31}P NMR (121 MHz, [D$_8$]toluene): δ = 69.1 (br., POH), –22.8 [br., P(O)H] ppm. ^{31}P NMR (162 MHz, CD_3OD): δ = 70.2 (quint, J_{P-F} = 26.7 Hz, POD) ppm. ^{31}P NMR (162 MHz, CF_3CD_2OD): δ = 72.8 (quint, J_{P-F} = 27.6 Hz, POD), –15.3 [t, J = 92.4 Hz, P(O)D], –15.0 [d, J = 606.0 Hz, P(O)H] ppm. IR (ATR): $\tilde{\nu}$ = 2402 (P–H) cm^{-1}.

2-(Diphenylphosphanyl)-2-propanol (6): A solution of diphenylphosphane oxide (**3**; 60 mg, 0.3 mmol) in acetone (1.5 mL) was concentrated to dryness in vacuo after 36 h of stirring at room temperature. Then the residue was dissolved in [D$_8$]THF (0.4 mL) at 50 °C. On cooling to room temperature, the product precipitated as colourless needles (20 mg, 26%). M.p. 125–127 °C. ^1H NMR (300 MHz, CD_2Cl_2/[D$_6$]acetone): δ = 7.88 (m, 4 H, C_6H_5), 7.28 (m, 6 H, C_6H_5), 3.01 (br., 1 H, OH), 1.19 (d, J = 13.4 Hz, 6 H, CH_3) ppm. ^{13}C NMR (75 MHz, CD_2Cl_2/[D$_6$]acetone): δ = 132.5 (d, J_{P-C} = 7.9 Hz, o-C_6H_5), 132.0 (d, J_{P-C} = 89.9 Hz, i-C_6H_5), 131.5 (d, J_{P-C} = 2.7 Hz, p-C_6H_5), 128.2 (d, J_{P-C} = 10.7 Hz, m-C_6H_5), 24.8 (d, J_{P-C} = 6.7 Hz, CH_3) ppm; C–OH signal not found. ^{31}P NMR (121 MHz, CD_2Cl_2/[D$_6$]acetone): δ = 31.3 ppm. $C_{15}H_{17}O_2P$ (260.27): calcd. C 69.22, H 6.58; found C 69.3, H 6.23.

X-ray Crystal Structure Analysis of 2: Data were collected with a STOE IPDS II diffractometer by using graphite-monochromated Mo-K_α radiation. The structure was solved by direct methods (SHELXS-97)[35] and refined by full-matrix least-squares techniques on F^2 (SHELXL-97).[35] XP (Bruker AXS) was used for graphical representations. $C_{14}H_{15}OP$, M_r = 230.23, orthorhombic, space group $P2_12_12_1$, a = 5.6391(11), b = 7.583(2), c = 28.459(6) Å, V = 1217.0(4) Å^3, Z = 4, $\rho_{calcd.}$ = 1.257 g cm^{-3}, μ = 0.201 mm^{-1}, T = 200 K, 17197 reflections measured, 2570 independent reflections (R_{int} = 0.0394) of which 2313 were observed [$I > 2\sigma(I)$], R_1 = 0.0279 [$I > 2\sigma(I)$], wR_2 = 0.0778 (all data), 151 refined parameters.

Acknowledgments

Financial support was provided by Evonik Oxeno GmbH. One of us (A. C.) is grateful for a research scholarship from the Degussa Stiftung. We thank Dr. O. Zayas, Mrs. H. Borgwald, Mrs. M. Geisendorf and Ms. K. Romeike for their skilled technical assistance. We also thank the group of Prof. Dr. M. Garland at the Institute for Chemical and Engineering Sciences (ICES) in Singapore for supporting the IR experiments and the application of BTEM. We thank PD Dr. B. Hoge (University of Cologne) for a generous gift of SPO **5** and valuable discussions.

[1] a) R. H. Crabtree, *The Organometallic Chemistry of Transition Metals*, Wiley, New York, **2001**; b) A. Börner (Ed.), *Phosphorus Ligands in Asymmetric Catalysis*, Wiley-VCH, Weinheim, **2008**, vol. I–III.
[2] a) D. M. Roundhill, P. R. Sperline, W. B. Beaulieu, *Coord. Chem. Rev.* **1978**, *26*, 263–279; b) B. Walther, *Coord. Chem. Rev.* **1984**, *60*, 67–105.
[3] a) M. Grayson, C. E. Farley, C. A. Streuli, *Tetrahedron* **1967**, *23*, 1065–1078; b) L. D. Quin, *A Guide to Organophosphorus Chemistry*, Wiley-Interscience, New York, **2000**.
[4] J. Chatt, B. T. Heaton, *J. Chem. Soc. A* **1968**, 2745–2757.
[5] N. V. Dubrovina, A. Börner, *Angew. Chem.* **2004**, *116*, 6007–6010; *Angew. Chem. Int. Ed.* **2004**, *43*, 5883–5886.
[6] For reviews, see: a) L. Ackermann, *Synthesis* **2006**, *10*, 1557–1571; b) L. Ackermann, *Synlett* **2007**, *4*, 507–526; c) L. Ackermann, R. Born, J. H. Spatz, A. Althammer, C. J. Gschrei, *Pure Appl. Chem.* **2006**, *78*, 209–214; d) L. Ackermann in *Phosphorus Ligands in Asymmetric Catalysis* (Ed.: A. Börner), Wiley-VCH, Weinheim, **2008**, vol. 2, pp. 831–847.
[7] For recent work, compare: a) L. Ackermann, *Synlett* **2007**, 507–526; b) A. Pfaltz, Y. Ribourdouille, X. Feng, B. Ramalingam, B. Pugin, F. Spindler WO2007135179 A1 20071129, **2007** (*Chem. Abstr.* **2007**, *148*, 11345); c) J. Bigeault, L. Giordano, I. de Riggi, Y. Gimbert, G. Buono, *Org. Lett.* **2007**, *9*, 3567–3570; d) J. Bigeault, I. de Riggi, Y. Gimbert, L. Giordano, G. Buono, *Synlett* **2008**, 1071–1075; e) B. Pugin, H. Landert, B. Gschwend, A. Pfaltz, F. Spindler WO 2009065783 A1 20090528, **2009** (*Chem. Abstr.* **2009**, *150*, 563987); f) L. Ackermann, S. Barfuesser, *Synlett* **2009**, 808–812.
[8] D. E. C. Corbridge, *Phosphorus: An Outline of its Chemistry, Biochemistry and Uses*, 5th ed., Elsevier, Amsterdam, **1995**, p. 336.
[9] a) Z. Luz, B. L. Silver, *J. Am. Chem. Soc.* **1961**, *83*, 4518–4521; b) J. Reuben, D. Samuel, B. L. Silver, *J. Am. Chem. Soc.* **1963**, *85*, 3093–3096; c) D. Samuel, *Pure Appl. Chem.* **1964**, *8*, 449–457; d) W. J. Bailey, R. B. Fox, *J. Org. Chem.* **1963**, *28*, 531–534; e) W. J. Bailey, R. B. Fox, *J. Org. Chem.* **1964**, *29*, 1013–1017; f) T. L. Emmick, R. L. Letsinger, *J. Am. Chem. Soc.* **1968**, *90*, 3459–3465.
[10] P. Nylen, *Z. Anorg. Allg. Chem.* **1938**, *235*, 161–182.
[11] N. B. Colthup, L. H. Daly, S. E. Wiberley, *Introduction to Infrared and Raman Spectroscopy*, Academic Press, New York, **1964**, pp. 299–300, 402.
[12] D. Magiera, A. Szmigielska, K. M. Pietrusiewicz, H. Duddeck, *Chirality* **2004**, *16*, 57–64.
[13] Yu. A. Ustynyuk, Yu. V. Babin, *Ross. Khim. Zh.* **2007**, *51*, 130–138.
[14] D. B. Chesnut, *Heteroat. Chem.* **2000**, *11*, 73–80.
[15] F. Wang, P. L. Polavarapu, *J. Org. Chem.* **2000**, *65*, 7561–7565.
[16] B. Hoge, S. Neufeind, S. Hettel, W. Wiebe, C. Thoesen, *J. Organomet. Chem.* **2005**, *690*, 2382–2387.
[17] The curve in the middle of Figure 1 was calculated by using B3LYP/6-31+G* [$\sigma(H_3PO_4)$ = 362.13 ppm, scaled onto $\delta(^{31}P)$ of H_3PO_4 (δ = 0 ppm)] and the lower curve by using GIAO-B3LYP/6-311+G*//B3LYP/6-311+G* [$\sigma(PPh_3)$ = 294.61 ppm, scaled onto $\delta(^{31}P)$ of PPh_3 (δ = –6.0 ppm)].
[18] For a review, see: I. A. Shuklov, N. V. Dubrovina, A. Börner, *Synlett* **2007**, 2925–2943.
[19] a) A. N. Chekhlov, *Zh. Strukt. Khim.* **2001**, *42*, 152–155 (russ.); b) A. Y. Garner, US 3346647, **1967** (*Chem. Abstr.* **1967**, *67*, 116943).
[20] Originally, this signal was attributed to the corresponding trivalent P–OH tautomer **3B**; see ref.[12]
[21] A similar conclusion was drawn by Hoge et al. from experiments considering the equilibrium between $(C_6F_5)_2P(O)H$ and

$(C_6F_5)_2POH$ carried out in the range between –70 °C and +50 °C in THF; see ref.[16]

[22] M. J. Frisch, G. W. Trucks, H. B. Schlegel, G. E. Scuseria, M. A. Robb, J. R. Cheeseman, J. A. Montgomery, Jr., T. Vreven, K. N. Kudin, J. C. Burant, J. M. Millam, S. S. Iyengar, J. Tomasi, V. Barone, B. Mennucci, M. Cossi, G. Scalmani, N. Rega, G. A. Petersson, H. Nakatsuji, M. Hada, M. Ehara, K. Toyota, R. Fukuda, J. Hasegawa, M. Ishida, T. Nakajima, Y. Honda, O. Kitao, H. Nakai, M. Klene, X. Li, J. E. Knox, H. P. Hratchian, J. B. Cross, C. Adamo, J. Jaramillo, R. Gomperts, R. E. Stratmann, O. Yazyev, A. J. Austin, R. Cammi, C. Pomelli, J. W. Ochterski, P. Y. Ayala, K. Morokuma, G. A. Voth, P. Salvador, J. J. Dannenberg, V. G. Zakrzewski, S. Dapprich, A. D. Daniels, M. C. Strain, O. Farkas, D. K. Malick, A. D. Rabuck, K. Raghavachari, J. B. Foresman, J. V. Ortiz, Q. Cui, A. G. Baboul, S. Clifford, J. Cioslowski, B. B. Stefanov, G. Liu, A. Liashenko, P. Piskorz, I. Komaromi, R. L. Martin, D. J. Fox, T. Keith, M. A. Al-Laham, C. Y. Peng, A. Nanayakkara, M. Challacombe, P. M. W. Gill, B. Johnson, W. Chen, M. W. Wong, C. Gonzalez, J. A. Pople, *Gaussian 03*, *Revision D.01*, Gaussian Inc., Wallingford, CT, **2004**.

[23] a) C. Lee, W. Yang, R. G. Parr, *Phys. Rev. B* **1988**, *37*, 785–789; b) A. D. Becke, *Phys. Rev. A* **1988**, *38*, 3098–3100; c) A. D. Becke, *J. Chem. Phys.* **1992**, *96*, 2155–2160; d) A. D. Becke, *J. Chem. Phys.* **1992**, *97*, 9173–9177; e) A. D. Becke, *J. Chem. Phys.* **1993**, *98*, 5648–5652.

[24] Calculated at the B3LYP/6-311+G* level of theory.

[25] R. C. Dobbie, B. P. Straughan, *Spectrochim. Acta, Part A* **1971**, *27*, 255–260.

[26] B. Hoge, P. Garcia, H. Willner, H. Oberhammer, *Chem. Eur. J.* **2006**, *12*, 3567–3574.

[27] The abrupt changes at 340 and 60°, respectively, can be rationalized by a slight change in the arrangement of the aromatic substituents as a result of a change in the dihedral angle.

[28] At room temperature a solution of $(C_5NF_4)_2POH$ (**5B**) in THF exhibited only a broad resonance for the OH group at δ = 9.03 ppm in the ^1H NMR spectrum, but with a decrease in temperature to 233 K a slight shift to a higher field was observed, and the signal was split into a doublet with J = 18.5 Hz. However, this doublet cannot be attributed to the existence of both P–OH rotational isomers, but is caused by a ^1H–^{31}P coupling (^2J). Owing to a fast exchange of the acid proton, this phenomenon is not observable at room temperature, but only at low temperatures when the mobility is decelerated. The same phenomenon is observed for many alcohols, e.g., methanol: H. Günther, *NMR-Spektroskopie – Eine Einführung*, Thieme, Stuttgart, **1973**.

[29] The measurement of the less stable SPOs **4** and **5** caused some problems. Thus, the absorption of $\tilde{\nu}_{PH}$ is very small. Also, other authors reported on this issue during the IR characterization of electron-poor phosphane oxides, for which no unequivocal bands for P–OH, P–H, or P=O vibrations could be observed: D. D. Magnelli, G. Tesi, I. U. Lowe, W. E. McQuistion, *Inorg. Chem.* **1966**, *5*, 457–461.

[30] The experimentally determined value of diphenylphosphane oxide (**3**) ($\tilde{\nu}_{PH}$ = 2368 cm^{-1}) is in accord with the value reported in the literature of $\tilde{\nu}_{PH}$ = 2370 cm^{-1}: J. Chatt, B. T. Heaton, *J. Chem. Soc. A* **1968**, 2745–2757.

[31] See the Exp. Sect. for further discussions on the pretreatment of data and BTEM analysis.

[32] This phenomenon is caused by intense solvent bands. For more details, see the Exp. Sect.

[33] The shoulder of $\tilde{\nu}_{OH\_1}$ and the bands at 3594 and 3685 cm^{-1} neither characterize compound **5B** nor traces of water. We attribute them to impurities and decomposition products.

[34] a) W. Chew, E. Widjaja, M. Garland, *Organometallics* **2002**, *21*, 1982–1990; b) E. Widjaja, C. Li, M. Garland, *Organometallics* **2002**, *21*, 1991–1997; c) M. Garland, *Mechanisms in Homogeneous Catalysis: A Spectroscopic Approach*, VCH-Wiley, Weinheim, **2005**.

[35] G. M. Sheldrick, *Acta Crystallogr., Sect. A* **2008**, *64*, 112–122.

[36] C. A. Busacca, J. C. Lorenz, N. Grinberg, N. Haddad, M. Hrapchak, B. Latli, H. Lee, P. Sabila, A. Saha, M. Sarvestani, S. Shen, R. Varsolona, X. Wei, C. H. Senanayake, *Org. Lett.* **2005**, *7*, 4277–4280.

[37] For the hydrolysis of P–Cl bonds with *t*BuOH, see: M. T. Reetz, T. Sell, R. Goddard, *Chimia* **2003**, *57*, 290–292.

Received: January 12, 2010
Published Online: April 7, 2010

